

# SPINAL CORD NEURONAL NETWORK SIMULATOR

Rogério R.L. Cisi and André F. Kohn  
University of São Paulo  
Biomedical Engineering Laboratory, EPUSP, PTC

## INTRODUCTION

A motoneuron pool in the spinal cord, associated with a given muscle, receives a multitude of neural commands from different parts of the central and peripheral nervous systems. The time course of the firing patterns of the motoneurons will define the dynamic behavior of the innervated muscle. The transformation of all synaptic inputs to the motoneuron pool onto muscle commands depends strongly on each motoneuron's intrinsic characteristics as well as on the associated neuronal network. As all involved relations are nonlinear, the functioning of the network has to be studied by simulation experiments. In a first stage, as described in this paper, our objective was to build a user-friendly simulator of a spinal cord neuronal network including a motoneuron pool, synaptic inputs from several sources (including the negative feedback due to Renshaw cells) and the generation of force by the associated muscle. There have been efforts described in the literature towards the development of spinal cord simulators (Maltenfort et al. 1998; Uchiyama et al. 2003), but usually the network simulator has been developed to answer a specific question and its general usability by a wider audience (without the need for programming) was not emphasized. In what follows we shall describe the structure of the neuronal network, the basic models employed for each element and the types of graphical analyses included in the simulator.

## METHODOLOGY

The simulated network structure is shown in Fig. 1. There are 272 motoneurons (MNs), with 70 type S, 62 type FR and 140 type FF, and 68 Renshaw cells (RC). The modeling was based mostly on available knowledge and data on cat gastrocnemius motoneurons and muscle fibers.

In the present version, relatively simple models were used for each element, so that the development of the network structure in an appropriate software environment could pave the way for future improvements of each element's model. This simplicity

was also deemed important for an overall analysis of the operation of the simulator, from the parameter setup phase to that when the results are graphed and analyzed.

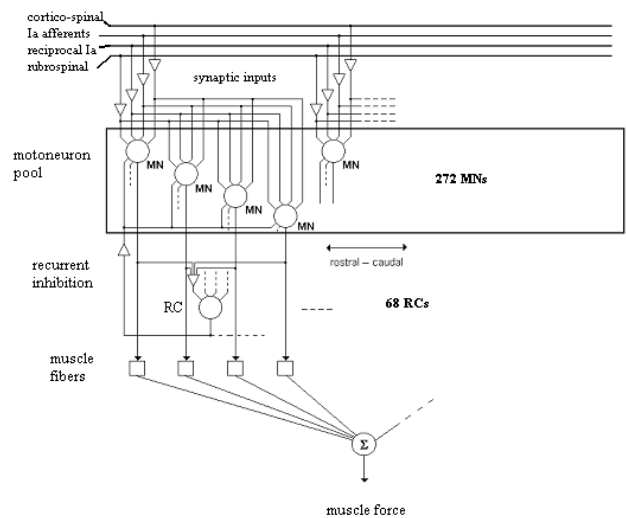


Fig. 1 – Structure of the simulated network.

The motoneuron pool receives synaptic inputs from a few independent pathways: cortico-spinal, rubrospinal (excitatory and inhibitory), Ia afferents, Ia reciprocal inhibition. Each of these inputs, if selected by the user, goes to all the MNs but with an effect that depends on each MN characteristics. The user may select either of two point processes for such inputs: Poisson or one with truncated Gaussian interspike interval with selectable mean and standard deviation. The former would mimic the superposition of many independent point processes while the latter could mimic the superposition of synchronized inputs. To mimic synaptic inputs that are independent from one MN to another, each MN also receives a lowpass filtered noise, with user selectable standard deviation and cutoff frequency.

Each motoneuron was modeled as a parallel association of a capacitance and several conductances in series with fixed voltage batteries. For

simplicity, the dendrites were not modeled in this first version, each presynaptic action potential affecting the motoneuron by a change in a single corresponding conductance, as described below.

Equations (1-5) describe the membrane potential of each motoneuron:

$$\frac{dV}{dt} = \frac{R}{\tau_{mem}} (I_{leak} + I_K + I_{syn} + I_{RC} + I_{sn}) \quad (1)$$

$$I_{leak}(t) = \frac{1}{R} (V_0 - V) \quad (2)$$

$$I_K(t) = G_K (V_K - V) \quad (3)$$

$$I_{syn}(t) = G_{syn} * (V_{syn} - V) \quad (4)$$

$$I_{RC}(t) = G_{RC} * (V_i - V) \quad (5)$$

where:

all potentials are with respect to the resting potential,  
 $V$  is the membrane potential,  
 $V_0$  is the leak potential, assumed equal to 0 mV,  
 $V_K$  is the potassium Nernst potential, taken as -10.0 mV,  
 $V_{syn}$  is the reversal potential for each synaptic input, equal to 70.0 mV for excitatory synapses and -16.0 mV for inhibitory,  
 $V_i = -16$  mV, the reversal potential of the Renshaw inhibitory synapses,  
 $R$  is the leak resistance,  
 $\tau_{mem}$  is the membrane time constant in the resting state,  
 $I_{leak}$  is the leakage current,  
 $I_K$  is the potassium current,  
 $I_{syn}$  represents any of the 4 synaptic inputs depicted in Fig. 1,  
 $I_{RC}$  is the current caused by the Renshaw cells,  
 $I_{sn}$  corresponds to the synaptic noise input, implemented as a lowpass filtered white noise  
 $G_{syn}$  are alpha functions corresponding to the synaptic input conductances of each MN.  
 $G_K$  is a two-exponential approximation to the four exponential proposal of (Baldissera and Gustafsson 1974), an example being shown in Fig. 2.  
 $G_{RC}$  is an alpha function conductance activated by the Renshaw cell inputs.

The three main types of motor units, S, FR and FF, found in mammals are modeled and included in the simulator. Whenever a MN fires a spike, there is a corresponding twitch on the respective muscle unit following an alpha function and an activation of Renshaw cells. These were modeled either by a fixed burst output, or by a parallel association of conductances with a time-varying potassium conductance. Each RC

was associated with 4 MNs on the same horizontal plane crossing the column of MNs running in the rostro-caudal

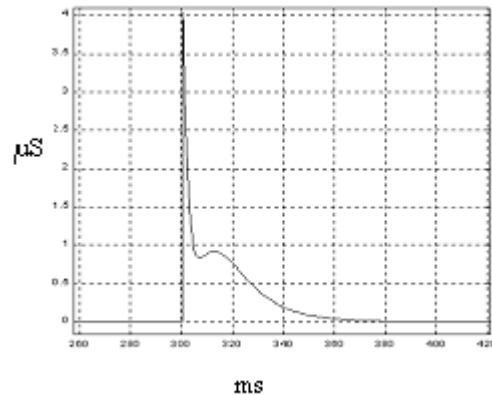


Fig. 2 – Potassium conductance following an action potential for FR type MN model.

direction in the spinal cord. Therefore, there were 68 planes, with the more caudal containing the S type MNs, the intermediate the FR type MNs and the more rostral planes containing the FF type MNs. The synaptic strength from a RC to a MN was maximum for the MNs in the same plane as the RC and decayed for MNs situated in planes on either side, with each RC limited to have a maximum span of 15 planes above and 15 below. On the other hand, each MN affects RCs on 2 planes above, 2 below and on the same plane, i.e., each MN affects 5 RCs. In the simple bursting RC model, each connected MN firing generates a burst (default duration: 40 ms) with a selectable discharge rate (default: 200/s). More refined bursting RC models could be included in future versions (Uchiyama et al. 2003).

The simulator may be subdivided in three parts: a parameter configuration module (with a set of default values and selectable standard deviations), an execution module and an analysis module. The configuration and analysis modules were developed in an event oriented concept using the Windows graphical interface. The execution module, which is the heart of the simulator, solves the differential equations of all the interconnected elements using a 4<sup>th</sup> order Runge-Kutta method. The development was done in the Microsoft Visual C++ 6.0 environment for both the execution module and the graphical interfacing. For the visualization of simulation results the following options have been included in the analysis module: the time evolution of several spike trains (the synaptic inputs, the motoneurons, the Renshaw cells); interspike interval histogram, spike rate versus time, membrane potential of a selected neuron; muscle force versus time. For a more refined signal processing or statistical analysis, the user may save

files in ASCII format of firing times, force and membrane potential.

RESULTS AND DISCUSSION

An example of a dialogue display used by the simulator during the network configuration phase is shown in Fig.3. The types and parameters of the desired synaptic inputs may be programmed using this screen. In the other screens, the user may modify the default parameter values of the MNs, RCs and muscle fibers.

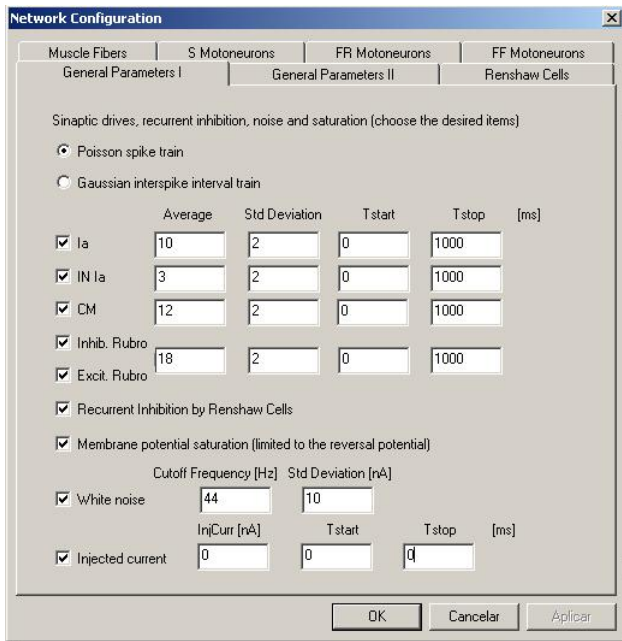


Fig. 3 – A configuration menu. The user may deselect any of the synaptic inputs and set parameter values for those selected.

After setting all desired parameter values and running the network, the user may choose different ways to show the results. Fig. 4 is an example of a graphical output, where the muscle force and the firing times of several motoneurons from the pool are shown. In this particular simulation the synaptic inputs to the 272 MNs were *i* an equivalent cortico-spinal Poisson spike train at 1000/s, *ii* the set of Renshaw cells and *iii* lowpass synaptic noise with cutoff frequency 44 Hz and 10 nA standard deviation. The RCs were run with the bursting model. This simulation used a step size of 0.05 ms and took about 3 min to run on a personal computer with 512 MB RAM and an Athlon XP 2400 processor (2 GHz clock).

The simulator has proved to be very user-friendly so researchers from the biomedical sciences should be able to use it with ease. The simulator is expected to be a helpful tool in theoretical and experimental studies on the neurophysiology of motor control. In particular, neurophysiological experiments on human motor control usually raise several hypotheses, which are not easy to test, due to the noninvasive character of the experiments. In such cases simulation experiments may be able to select the most probable hypothesis.

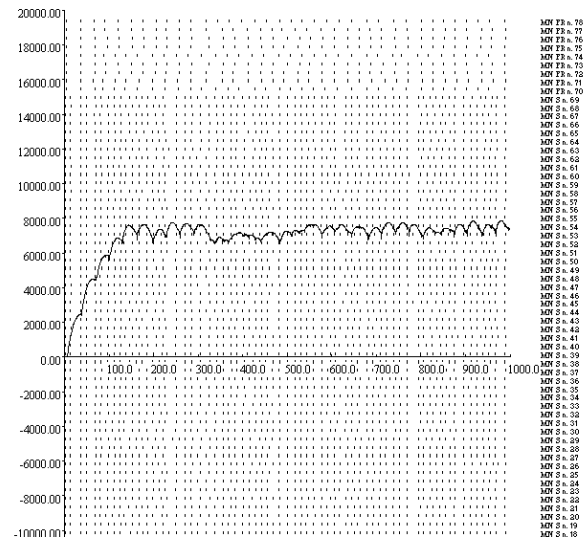


Fig. 4 – Force (gram-force) as a function of time (ms) and discharges of several MNs, each discharge indicated by a small vertical bar.

REFERENCES

Baldissera, F. and B. Gustafsson (1974). "Afterhyperpolarization Conductance Time Course in Lumbar Motoneurons of Cat." *Acta Physiologica Scandinavica* **91**(4): 512-527.

Maltenfort, M. G., C. J. Heckman and W. Z. Rymer (1998). "Decorrelating actions of Renshaw interneurons on the firing of spinal motoneurons within a motor nucleus: a simulation study." *J. Neurophysiology* **80**: 309-323.

Uchiyama, T., H. Johansson and U. Windhorst (2003). "A model of the feline medial gastrocnemius motoneuron-muscle system subjected to recurrent inhibition." *Biol. Cybern.* **89**: 139-151.